IPPI

Polyolefins Journal, Vol. 9, No. 2 (2022)
DOI: 10.22063/POJ.2022.3112.1211

ORIGINAL PAPER

Nitroxide-mediated radical polymerization of styrene from poly(ethylene terephthalate) and its polymer/montmorillonite nanocomposite

Saber Ghasemi Karaj-Abad[1*], Lily Sadr[1], Mojtaba Abbasian[2], Mehdi Hosseinzadeh[*3], Solmaz Esmaeily Shoja[4], Mehdi Jaymand[5]

[1]Department of Chemistry, Payame Noor University, P. O. Box: 19395-3697 Tehran-Iran
[2]Department of Chemical Engineering, University of Bonab, Bonab, Iran
[3]Marand Faculty of Technical and Engineering, University of Tabriz, Tabriz, Iran
[4]Lab. of Materials, Faculty of Engineering, Islamic Azad University, Bonab branch, Bonab, Iran
[5]Nano Drug Delivery Research Center, Health Technology Institute, Kermanshah University of Medical Sciences, Kermanshah, Iran

Received: 3 February 2022, Accepted: 29 May 2022

ABSTRACT

In this study, for the first time, a novel strategy for the synthesis of graft copolymers using polystyrene (PSt) monomer from surface modification of poly(ethylene terephthalate) PET through surface-initiated nitroxide-mediated radical polymerization was performed. For this purpose, the PET surface was first aminated by 1,3-diamino propane, which was used as an amination agent. Second, phenyl chloro acetylation of PET was prepared by coupling amino and hydroxyl groups with α-phenyl chloro acetyl chloride. Afterward, 2,2,6,6-tetramethyl-1-piperidinyloxy (TEMPO) was synthesized, then 1-hydroxy-2,2,6,6-tetramethylpiperidine (TEMPO–OH) was obtained by reduction of TEMPO with sodium ascorbate and coupled with chloroacetylated PET to obtain PET-TEMPO macroinitiator. Furthermore, the (St) monomer was grafted onto the PET surfaces through the "grafting from" technique. The obtained macroinitiator for living radical polymerization was heated in the adjacency of (St) monomer to obtain the graft copolymer (PET-*g*-PSt) onto the PET surfaces. Finally, PET-*g*-PSt/MMt nanocomposite was synthesized by the solution intercalation method. The surface combination, morphology, and thermal properties of the modified PET films were proved using various characterization methods such as transform infrared spectroscopy (FT-IR), ^{1}H nuclear magnetic resonance (^{1}H NMR), differential scanning calorimetry (DSC), thermogravimetric analysis, X-ray photoelectron spectroscopy, and termination electron microscopy (TEM). **Polyolefins J (2022) 9: 163-174**

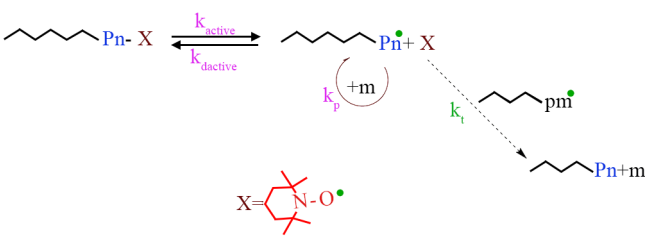
Keywords: Nitroxide-mediated radical polymerization (NMRP); TEMPO; poly(ethylene terephthalate) (PET); surface-initiated polymerization; graft copolymer.

INTRODUCTION

Poly(ethylene terephthalate) (PET) film is a most abundant class of semi-crystalline thermoplastic polyesters with vast stability, visibility, electrical insulation, exhaustion resistivity, and weather persistence; these extraordinary basic features have led to a broad range of industrial and economic applications [1] for example X-ray, molding resins, and photographic films. This polymer is created in significant quantities and can be discovered and used in various industries, such as the textile industry, high stability fibers, printing papers, magnetic tape, packaging, medical and pharmaceutical fields [2]. The functional surface of PET film is significant in special applications such as biocompatible materials, conductive films, and packing films [3-5]. However, multiple hydrophobic property, low surface power, and weak coherence of PET surface, that are owing

*Corresponding Author - E-mail: Mehdi Hosseinzadeh: mh_1268@yahoo.com; Saber Ghasemi Karaj-Abad: sg.chemist1988@gmail.com, ghasemi_s@yahoo.com

to the absence of polar groups such as carboxyl and hydroxyl in its structural molecules, constrain its performance as a biocompatible and viable material for lesion healing and culture cells [6-8]. A typical way to advance surface activation is through modification. To modify excellent features of PET surface and expand its applications, the explanation and presentation of special functional groups onto PET surface have been extensively investigated using physical or chemical procedures. On the other hand, one of the most efficient techniques for PET surface modification is the immobility of polymer chains on the PET surface by grafting-from or grafting-to, which have been recently developed [9,10]. There are several methods for this purpose; one of the remarkable methods, in this case, is grafting from PET. Anionic, cationic, ring-opening, and radical procedures have been employed to provide graft copolymerization of PET as a surface [10-16]. For example, PET was grafted with styrene (St) using synchronous radiance method through X-ray [17]. It was found that the degree of grafting was highly dependent on the grafting parameters wherein the features of the chemical, structural, and thermal properties of poly(ethylene terephthalate)/polystyrene (PET-*g*-PSt) were extensively studied [18]. The swiftly progressing field of living/free radical polymerization provides further achievements for grafting copolymers with a defined structure. In living radical polymerization, the concentration of growing radicals is suppressed to avoid termination. This is made feasible by applying multiple means such as iniferters (TEMPO) [19,20], degenerative transition, organometallic species, and atom transition [21,22]. For this reason, one of the most significant achievements is the growth of living free radical polymerization and the preparation of synthetic polymers with narrow polydispersity and predetermined molecular weight [23,24]. Furthermore, one of the most appropriate techniques for performing such chemistry is employing TEMPO as a chain-end



Scheme 1. Mechanism for nitroxide-mediated polymerization.

counter-radical to intercede the polymerization of styrene derivatives, also acrylate and styrene [20].

Considering this conceptual viewpoint, RDRP, which is commonly known as living/free radical polymerization (LFRP), including reversible addition of fragmentation chain transfer (RAFT) polymerization [25,26], atom transfer radical polymerization (ATRP) [27,28], and nitroxide-mediated polymerization (NMP) [29,30], has been considered as a strong evidence for the synthesise of macromolecules with predetermined molecular weight distribution as well as narrow dispersity (MWD or M_w/M_n). Among these techniques, NMP was developed and applied in 1984, and is essentially the simplest RDRP technology to use in this class of polymerization approach. This approach is a basic and widely used approach that can be used in homogeneous and heterogeneous environments due to its applicability in a broader range of monomers (eg, acrylates, acrylamides and vinyl chloride) [31,32]. Basically, this polymerization method is applied to a conventional radical initiator (e.g., benzoyl peroxide) with the emergence of a stable nitroxide radical (e.g., TEMPO) or alkoxyamine radical, which is assigned to the preparation of graft copolymers and star under mild situations [33,34]. On the other hand, grafting copolymers with vinyl monomers on plastics in homogeneous media is an effective way to develop and modify the range of useful plastics. However, compared with other graft copolymerizations, an advantage of 'living' free radical polymerization (LREP) is that, the terminal groups are quietly constant at room temperature and prepolymers can be insulated, reserved, and applied as required. Furthermore, for this kind of polymerization, stringent polymerizations conditions are required.

The mechanism of living polymerization consists of the following steps: (1) thermally impelled homolytic carbon-oxygen fragmentation of alkoxyamine (C-ON) bond to obtain polystyryl radical and nitroxyl counter-radical; (2) propagation through the addition of monomer to polystyryl radical, which is created in step 1; and (3) chain-capping with propagating species using the recombination of TEMPO free radical (Scheme 1).

In recent decades, many types of research on the preparation of organic–inorganic nanocomposites have been extensively reviewed due to their extraor-

dinary mechanical, thermal, optical, electrical features and wide-spreading potential applications as developed functional materials [35,36]. On the other hand, polymer/clay nanocomposites (PCNs) in current investigation are of special interest due to their small size and developed physicochemical characteristics. These intrinsic and extraordinary features have made nanocomposite materials have a vital role to play in the sustainability of advanced nanomaterial that have not been discovered in conventional composites and natural polymers [37,38]. Furthermore, these nanocomposites display advanced fire retardancy, gas barrier properties, corrosion persistence, developed thermal stability, ionic conductivities, mechanical ability or optical features, and reduced absorbance in organic fluids [36]. Among these kinds of obtained materials, preparation of nanocomposites based on PET can be considered as a low-cost, reproducible and viable property. Furthermore, these materials can be environmentally friendly due to their alternative and favorable properties. Also, these materials with extensive and various applications can play an important role in the synthesis of polymer materials [39,40]. In the present study, for the first time, nitroxide mediated radical polymerization was used for grafting copolymerization of a hydrophobic monomer (St) on PET surface to obtain exfoliated and intercalated PET-*g*-PSt/clay nanocomposites with excellent barrier features. The approach is to combine both passive barrier and active barrier approaches by modifying pristine clay with trade name Cloisite NaC, which possesses the idealized chemical formula $Na_{0.33}[Mg_{0.33}Al_{11.67}Si_4O_{10}](OH)_2$ with long-chain fatty acids, and blending these nanoparticles with PET to make nanocomposites with excellent barrier features. The results presented here are preliminary investigations into the polymerization of styrene monomer from surface modification of PET through surface-initiated nitroxide mediated radical polymerization. The next step of this work will be to prepare composite polymers and new materials by surface polymerization of PET and compare the results with those obtained previously by different methods [41,42]. Accordingly, it is noteworthy that the prepared PET-*g*-PSt copolymer and its attributed nanocomposite are possibly used as reinforcing agents in the preparation of composite polymers, also in the packaging and membrane materials due to combination of PSt and PET and synergetic application of MMT. For this purpose, first, PET surface aminated by 1,3-diamino propane was used as the amination agent. Second, phenyl chloro acetylation of PET was performed by coupling amino and hydroxyl groups with α-phenyl chloro acetyl chloride. Afterward, TEMPO–OH was obtained by reducing TEMPO with sodium ascorbate and coupling with chloroacetylated PET to obtain a PET-TEMPO macroinitiator. Styrene (St) monomer was then grafted from PET surfaces by the NMP method. Finally, the obtained PET-*g*-PSt copolymer was converted to nanocomposite as filler by increasing the content of organoclay (modified montmorillonite (O-MMT); 2 wt%). To our knowledge, this is the first detailed report on TEMPO-mediated graft polymerization of St monomer from PET surface and its polymer/clay nanocomposite synthesis.

EXPERIMENTAL

Materials

Polyethylene terephthalate (PET) films of dimension 6 cm × 6 cm and 0.1 mm thickness were attained from Shahid Tondgooyan Petrochemical Co., Iran, and were washed several times with cold methanol/acetone (50/50 vol %) and dried before use. α-Phenyl chloro acetyl chloride was used as received without further purification. Methanol and dichloromethane were respectively purchased from Merck and Aldrich and used without purification. Styrene was obtained from Tabriz Petrochemical Co., Iran, and purified under reduced pressure before use. TEMPO and O-MMT were synthesized by a research team in our laboratory [42,44]. Triethylamine was distilled and purified on calcium hydride before use. Tetrahydrofuran (anhydrous, 99.9%) was obtained from Merck and dried by reflexing over a sodium benzophenone complex (the profound purple color displayed a moisture-free solvent). All other solvents and reagents were acquired from Sigma-Aldrich and Merck and directly utilized according to the literature.

Instrumentation

FT-IR spectrum was collected using Shimadzu FTIR-

8101M (Kyoto, Shimadzu, Japan) within the wavenumbers ranging from 400 to 4000 cm^{-1}, with an attenuated whole reflection instrument. To prepare the specimens, the dry powders were grounded with potassium bromide (KBr) powder and the admixture was compressed into form disks. The disks were reserved in a desiccator to avoid humidity absorption. Proton nuclear magnetic resonance (^1H NMR) spectrum was obtained at 25°C by applying an FT-NMR (400 MHz) Brucker spectrometer (Germany, Brucker, Ettlingen). The specimen was obtained for ^1H NMR spectroscopy on Varian INOVA-500 (Palo Alto, CA, USA) by dissolving about 10 mg of the sample in 5 ml of deuterated chloroform ($CDCl_3$) or dimethyl sulfoxide (DMSO-d6), and chemical shifts were confirmed in ppm units with tetramethylsilane (TMS) as an internal standard. The thermal properties of the graft copolymers and synthesized nanocomposite were performed by a thermogravimetric analyzer (TGA-METTLER/TOLEDO-SDTA 851e; Polymer Laboratories, UK, Shropshire). In thermogravimetric analysis (TGA) examinations, nearly 10 mg of the specimens were obtained under a flow of nitrogen gas from 25°C to 600°C with a heat rating of 10°Cmin^{-1}. Differential scanning calorimetry (DSC) analyses were performed with a NETZSCH (Germany, Selb)-DSC 200 F3 Maia. The specimen was first heated to 200°C and then cooled for 5 min to remove the thermal history. Afterward, the specimen was exposed to heat again, up to 200°C at a rate of 10°Cmin^{-1}. The entire testing was carried out under a flowing nitrogen atmosphere at a flow rating of 50 ml min^{-1}. The spectrum of X-ray diffraction (XRD) was recorded with a Siemens D 5000 X-ray generator (Cu Ka radiation with k = 1.5406 Å) by scanning 2θ in the range of 2 to 30°C at 25°C. Transmission electron microscopy (TEM) was carried out using a Philips CM10-TH microscope (Netherlands, Phillips, Eindhoven) with a 100-kV accelerator voltage.

Synthesis of PET- NH_2

In a 100-mL two-necked round-bottom flask equipped with a refluxing condenser, a magnetic stirring, septum and gas inlet/outlet, PET (around 100 mg) film was plunged into the flask containing 1,3-diaminopropane solution in cold methanol (1 M), which was previously thermostated in an oil bath . During the reaction, mild agitation was applied. The PET film was eliminated after the grafting reaction, washed with cold methanol several times and dried in reduced pressure at room temperature for at least 12 hours.

Synthesis of PET- Cl

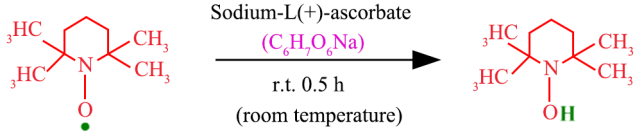
To achieve the chloroacetylated PET, amino-functionalized PET surfaces were successfully treated with α-phenyl chloroacetyl chloride in the presence of triethylamine in THF as solvent. To obtain this objective, amino-functionalized surfaces were plunged into 7 mL of anhydrous THF. Furthermore, to attain dispersion, triethylamine (0.3 mL, 4.3 mmol) and α-phenyl chloroacetyl chloride (0.1 mL, 1.2 mmol) were added to the flask. A large excess of α-phenyl chloroacetyl chloride was used compared to amino groups. After this time, the reaction was gently stirred overnight. The functionalized PET surfaces were then purified by repeated washing with water, THF and dichloromethane and dried in vacuum at room temperature. Finally, the reaction mixture under reduced pressure at 25°C was dried and carried out a second time to produce a quantitative product.

Preparation of TEMPO–OH by reduction of TEMPO

The reduction of TEMPO to TEMP-OH under the influence of sodium ascorbate was accomplished as follows. In summary, TEMPO (2 g, 7.5 mmol) was plunged into a solution of sodium ascorbate (2.5 g, 11.6 mmol) in water (18 mL) and shaken severely until it was completely decolorized (ca. 0.5 h). The resulting suspension was extracted with ether, washed with brine and water, then dried over sodium sulfate (Na_2SO_4) and vaporized by applying a rotary vaporizer to obtain TEMPO–OH (0.84 g (80%)). (Scheme 2).

Synthesis of PET–TEMPO macroinitiator

A 50-mL flask containing TEMPO-OH (95 mg, 0.608 mmol) and anhydrous THF (3 ml) was fitted with a condenser refluxing, a magnetic stirrer, and a gas inlet/



Scheme 2. Synthesis of TEMP-OH. TEMP-OH: 1-hydroxy-2, 2, 6, 6-tetramethylpiperidine.

outlet. The reaction mixture was attached to the argon gas line, and then NaH (90 mg, 70% dispersion in oil, 3 mmol) was added to the reaction mixture and stirred under argon atmosphere for 30 min at room temperature. After that, a solution of PET-Cl (250 mg) in THF (20 ml) was added drop-wise to the reaction mixture. The reaction mixture was heated at reflux under argon atmosphere for about 12 hours, then cooled and compressed to dry. The residue was dissolved in CH_2Cl_2 (160 ml), then washed several times with ice/water, and dried. Finally, the crude yield was purified thrice by precipitation from a solution in excess CH_2Cl_2 and cold methanol to produce the TEMPO-functionalized polymer as a whitish solid (300 mg).

Synthesis of PET-*g*-PSt

The reaction mixture of macroinitiator (0.045 g) and styrene (2 g, 20 mmol) was charged in a polymerization ampoule. The ampoule was degassed (three freeze-pump-thaw cycles), sealed off under a vacuum, and placed in an oil bath at 125°C for about 4 hours. During this time, the polymerization mixture became gradually stickier and stiffer. Finally, the yield was dissolved in CH_2Cl_2 and was precipitated and filtered into ice methanol. The separation of PET-*g*-PSt from PSt (perhaps thermally formed) was performed in part according to a process proposed by Xie and coworkers [45]. Furthermore, to eliminate PSt, the crude yield was extracted several times with cyclohexane at 30°C. The purified yield was dried in a vacuum and weighed. The PET-*g*-PSt graft copolymer was produced as a whitish solid (0.160 g) (Scheme 3).

Extent of grafting

The PET-*g*-PSt specimens were extracted with cyclohexane for 3 h in a Soxhlet extraction instrument, purified and dried in a vacuum for 24 h. The extent of grafting was calculated by the following equation and is 2.5 % (46).

$$\%\text{grafting (G)} = \frac{\text{weight of PET - } g \text{ - PSt} - \text{weight of PSt}}{\text{weight of crude PET - } g \text{ - PSt}} \times 100 \qquad (1)$$

Synthesis of PET-*g*-PSt /MMT nanocomposite via solution intercalation method

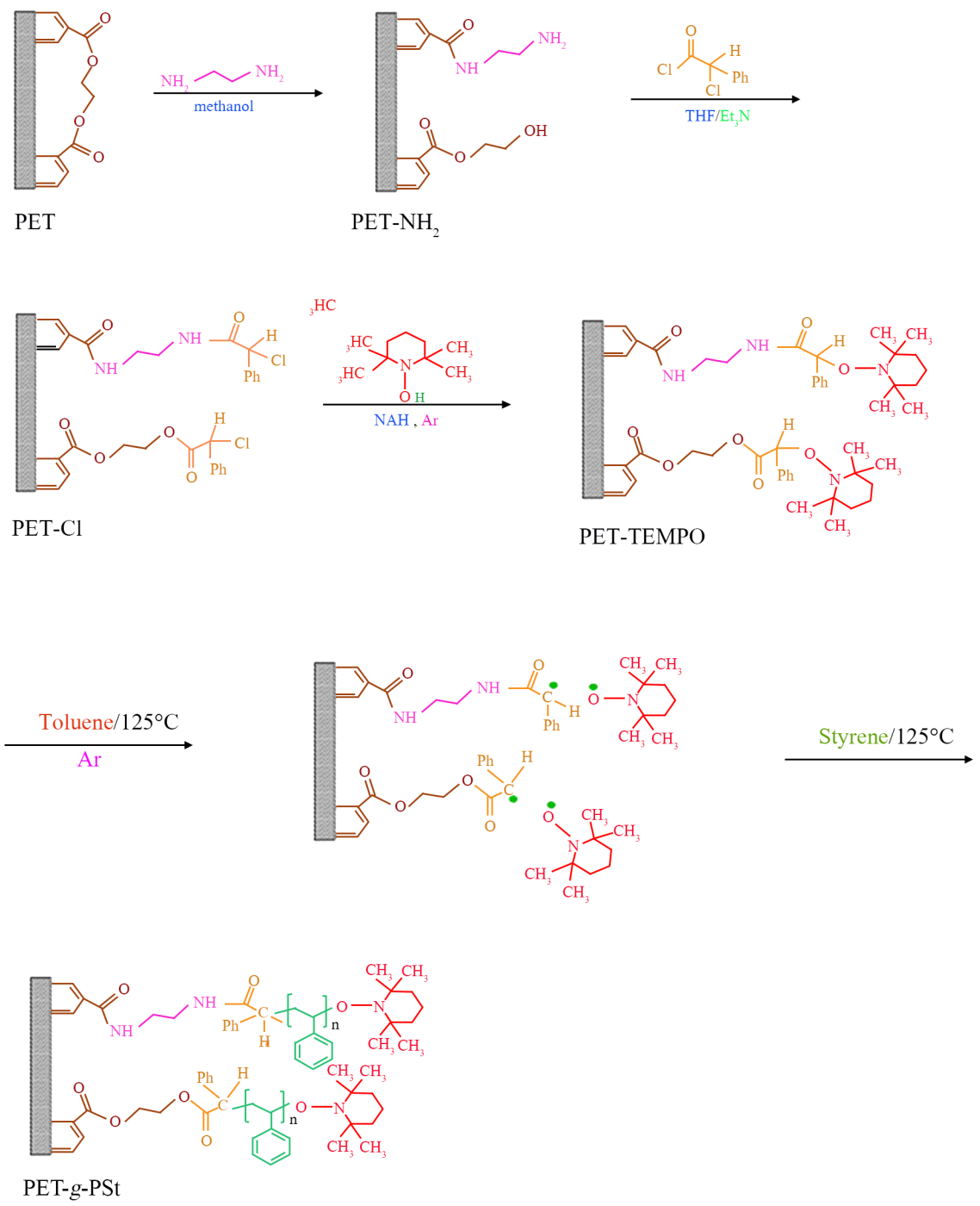
O-MMT (0.02 g, 2 wt %) was dispersed in 30 mL of toluene under sonication for about 20 minutes. In another vessel, the prepared PET-*g*-PSt (0.160 g) was dissolved in 40 mL of toluene. Next, the clay suspension was added drop-wise to the polymer solution while stirring for approximately 12 hours at 50°C. Afterward, the mixture was plunged into ice methanol (400 mL) for swift precipitation. The precipitate was purged and dried in reduced pressure at 25°C.

RESULTS AND DISCUSSION

Investigation of FT-IR spectroscopy

The FT-IR spectra of neat PET, PET-NH_2, PET-Cl, PET-*g*-PSt, and PET-*g*-PSt/MMT nanocomposite are presented in Figure 1. According to the spectra of neat PET film, the stretch vibration of the R′COOR group was observed at 1711 and 755 cm^{-1}. Also, the symmetric and asymmetric stretch vibration of the CH_2 group of C_2H_4 were observed at 2854 and 2972 cm^{-1}, respectively. The stretch vibration of ACOH was observed at 3050 cm^{-1}, which is due to the presence of benzene ring and the stretch vibration of skeletal CAC in-plane was observed at 1505 and 1600 cm^{-1}, respectively. The absorption peak at 859 cm^{-1} is attributable to the para substitution of the benzene ring. The FTIR spectra of PET- NH_2 displays an absorption band at 3554 cm^{-1}, which is attributed to the coupling between the NH and OH. According to the FT-IR spectrum of PET-Cl, a sharp absorption peak at 727 cm^{-1} corresponds to the stretch bond of C-Cl, and an absorption peak at 1727 cm^{-1} is assigned to the stretch bond of the carbonyl group. Also, the intense decrease of the absorption band at 3546 cm^{-1} verifies the chlorination of amino-functionalized PET surfaces.

The FTIR spectra of PET-*g*-PSt exhibited the characteristics of absorption peaks, including stretch vibration of C-H at 3100-2800 cm^{-1}, stretching vibrations of C-H at 1435 and 1354 cm^{-1}, weakly aromatic overtone, and composition peaks in the 1900-1650 cm^{-1}. After polymerization of styrene onto neat PET, a novel peak at 725 cm^{-1} is revealed, which is attributed to the aromatic structure of grafted polystyrene. The severity of this peak enhances by increasing the polymerization time. Also, the symmetric stretching of OCHO of the polystyrene was observed at 2977 cm^{-1}. In addition, the ROH groups of the PET surface and absorbed water



Scheme 3. Synthetic route for the grafting of NMRP initiators and styrene polymerization on the PET surfaces.

molecules using the PET surface were centered at about 3341 cm^{-1}. The spectra of PET-*g*-PSt /MMT nanocomposite exhibited the characteristics absorption peaks, including aromatic C=C stretch vibration at 1452, 1492, and 1600 cm^{-1}, aromatic C-H at 3059 cm^{-1}, and grafting of Si-O montmorillonite in the area of 1025-1056 cm^{-1}.

Graft Copolymerization

The PET-TEMPO macroinitiator was applied for NMP of styrene onto the PET surfaces. Figure 2 indicates the ^{1}H NMR spectrum of PET-g-PSt and neat PET. In the ^{1}H NMR spectra of neat PET, two areas were clearly visible. The peaks appearing in the 4.3 ppm area are attributed to the aliphatic protons of the methyl groups, as well as aromatic protons of the benzene

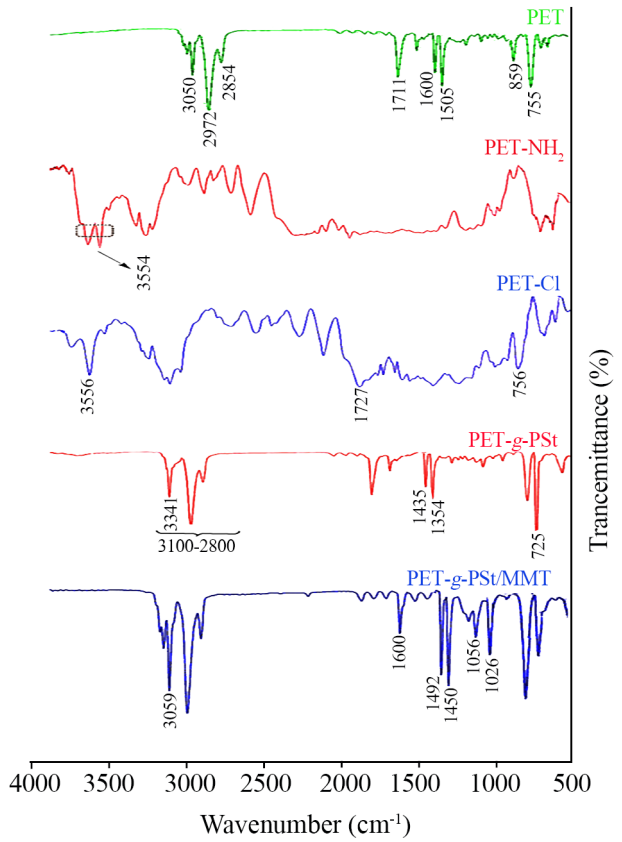


Figure 1. FTIR spectrum of net PET, PET-NH_2, PET-Cl, PET-g-PSt, and PET-*g*-PSt /MMT nanocomposite.

rings in the 7.5 ppm range. The chemical shifts of aromatic and aliphatic protons of PSt side chains in the ^{1}H NMR spectrum of PET-*g*-PSt/MMT nanocomposite were observed at 6.35-7.00 and 2.25-2.95 ppm, respectively. Also, after polymerization, the chemical shifts related to the $-CH_3$ and $-CH_2$ groups of TEMPO appeared at 1.30 ppm. In addition, the chemical shifts of phenyl protons of the macroinitiator are observed at 6.9-7.25 ppm. Analysis discussion demonstrated that the graft copolymerization of styrene onto the PET surface by NMP was performed. In addition, a graft copolymer of PET with PSt was also attained by NMP of PET-*g*-PSt containing active terminal nitroxide. These results demonstrate that the polymerization proceeds via NMRP.

Investigation of PET-*g*-PSt/MMT nanocomposite

The thermal behaviours of neat PET, PET-*g*-PSt copolymer, and PET-*g*-PSt/MMT nanocomposite were investigated using DSC and TGA curves, as seen in Figures 3 and 4. As seen, the glass transition temperature (T_g) of neat PET is 70°C, and the melting temperature (T_m) is equal to 250°C. The DSC curve of PET-*g*-PSt copolymer displayed an endothermic peak at approximately 95°C and 150°C, which is attributed to the T_g of the graft copolymerization of polystyrene. On the other hand, the T_g value of the PET-*g*-PSt/MMT nanocomposite, partially shifted to a higher temperature, appeared at 130°C. This procedure is probably due to the nanoscale extent dispersion of silicate layers into the PET-*g*-PSt matrix, as well as due to the s trong interfacial action and reaction between the polymer chains and clay layers. This indicates the separation of the polymer microphase, and in this copolymer our two monomers (PET and PSt) are immiscible.

On the other hand, the thermal performance of the neat PET, prepared PET-g-PSt copolymer and its polymer/clay nanocomposite under nitrogen protection was studied using TGA analysis (Figure 4). The characteristic TGA analysis of the PET-*g*-PSt copolymer indicates that the graft copolymer's degradation started at 350°C temperature, and the very mild increase in degradation rate continues until 460°C temperature, after a while, the loss rate slows down. The residue at 600°C for the prepared PET-*g*-PSt copolymer is approximately 10 wt%.

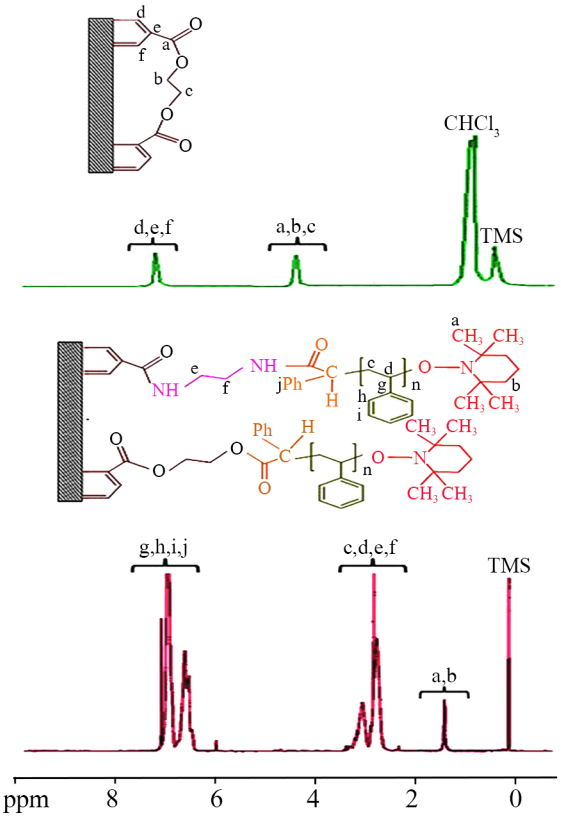


Figure 2. ^{1}HNMR spectra of neat PET and PET-*g*-PSt.

But, the TGA trace of PET-*g*-PSt/MMT nanocomposite was degraded using a single degradation step around 400-490°C, and after a while, the loss rate slowed down. The residue at 600°C for this sample is approximately 12 wt%. Further degradation occurred in the area between 150-300°C. This area is owing to the dehydration of the clay followed by primary degradation of the hexadecyl trimethyl ammonium salt. It is noteworthy that the enhancement in the terminal product of nanocomposite compared to the pristine PET-*g*-PSt copolymer indicates a decrease in the inflammability of the polymer, and this proves the excellent thermal stability of the prepared nanocomposite. As a result, compared with pristine PET-*g*-PSt copolymer, the synthesized nanocomposite illustrated higher thermal stability. Nevertheless, the increased thermal stability of polymer/clay nanocomposite is demonstrated through the formation of clay, which functions as a mass transportation hindrance and isolator between the new polymer and the negligible area where the copolymer decomposition is performed.

It is clear that TEM represents a factual image of the morphology of the prepared nanocomposite. The TEM image of PET-*g*-PSt/MMT nanocomposite with 2-wt% clay load is displayed in Figure 5. As seen in Figure 5, the clear and light areas are attributable to the polymer matrix, and the black parts are attributed to the silicate layers. As predicted, silicate layers were randomly dispersed within the PET-*g*-PSt matrix, and multilayer morphology has been lost between silicate layers. Therefore, the intercalation and exfoliation

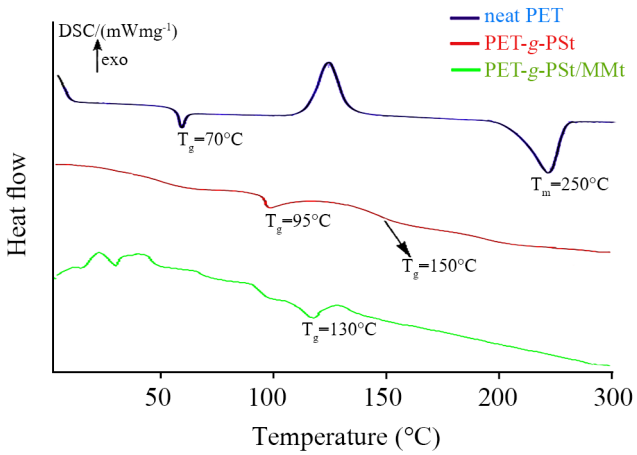


Figure 3. DSC traces of neat PET, PET-*g*-PSt, and PET-*g*-PSt /MMT nanocomposite.

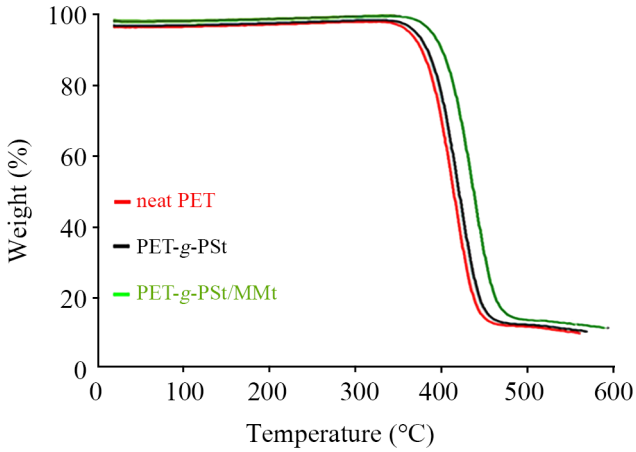


Figure 4. TGA curves of neat PET, PET-*g*-PSt and PET-*g*-PSt /MMT nanocomposite.

of the clay materials within the polymer matrix are proved. In addition, a small number of clay layers accumulate. Furthermore, some larger intercalated layers can also be recognized. On the other hand, in Figure 5, the accumulation of MMT nanoparticles can be figured out at different levels, which may be attributable to incorporated or slightly exfoliated structures. Nevertheless, the clay is not fully distributed in the polymer matrix. The thin areas display only layers of the lost clay particles, which signifies the exfoliation structure. If the silicates are homogeneously and randomly distributed in the polymer matrix, as a result, the jointing area is vast, and noticeable interaction can be envisaged.

XRD investigation of O-MMT and PET-*g*-PSt/MMT nanocomposite

The XRD patterns of neat MMT and O-MMT are shown in Figure 6. As seen, the intercalation spacing of O-MMT is significantly increased compared to the neat MMT, which resulted in a variation in the X-ray diffraction peak towards a lower angle. The parameters were estimated from the appeared peaks of the angular situation 2θ using the Bragg formula: $n\lambda=d\sin\theta$. The XRD data display the wide peak centre at d = 1.4 nm attributed to MMT, which has converted to a new peak at 1.10 nm. It can be concluded from these XRD patterns that the alkylammonium ions have been incorporated into the MMT layers.

On the other hand, the XRD patterns of neat PET and PET-*g*-PSt /MMT nanocomposite are shown in Figure 7. As observed in the XRD patterns of neat PET, the peak that appears at 2θ =10 is related to neat poly-

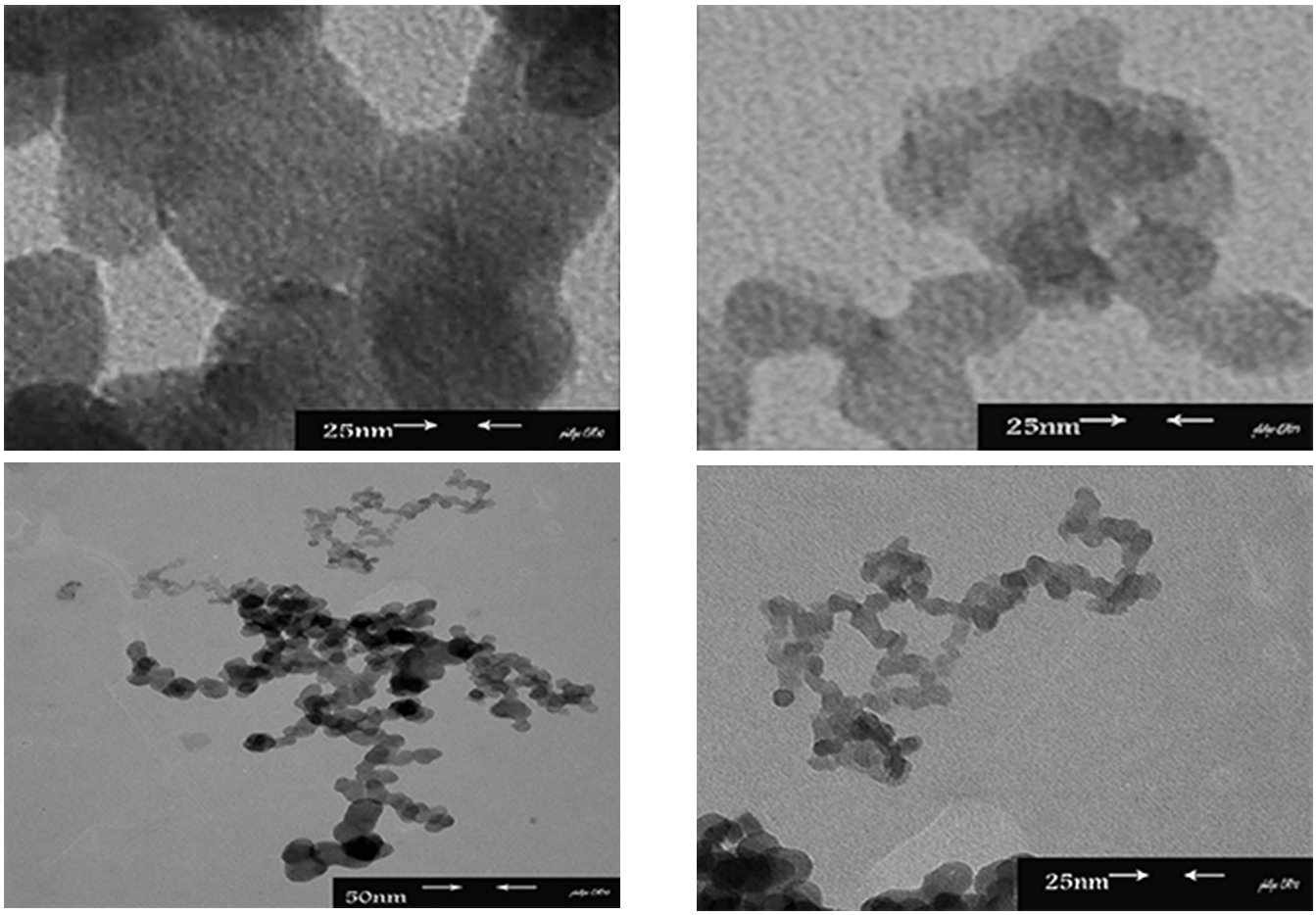


Figure 5. TEM images of PET-*g*-PSt/MMT nanocomposite.

ethylene terephthalate. Polyethylene terephthalate is highly amorphous and has low crystallization ability. Furthermore, the XRD pattern of O-MMT and synthesized polymeric nanocomposite reveals that the peak that appeared at 2θ =3 in the case of O-MMT has completely disappeared in the case of polymeric nanocomposite due to the preparation of nanocomposite by a solution intercalation method. This peak elimination indicates that polymer chains effectively have been able to penetrate between the clay layers and the clay structure is disintegrated. In conclusion, the resulting structure is disintegrated, which in some ways superior

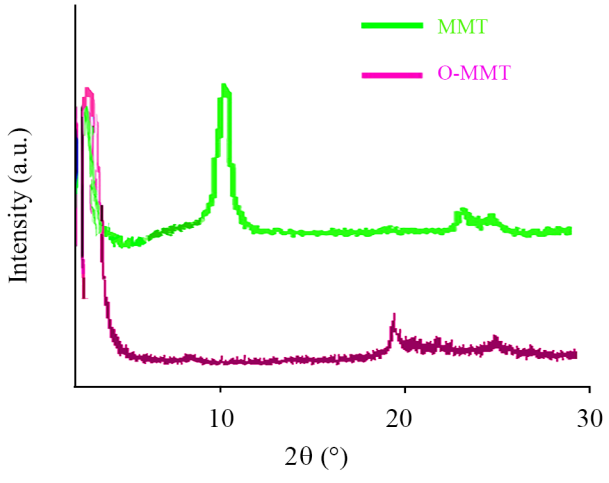


Figure 6. XRD patterns of MMT and O-MMT.

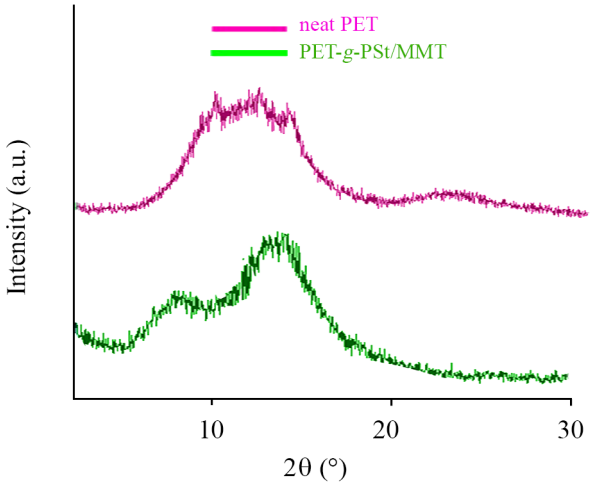


Figure 7. XRD patterns of net PET (a) and PET-*g*-PSt /MMT nanocomposite (b).

to other structures. For example, the thermal stability of disintegrated nanocomposites is usually better than that of interlayer nanocomposites [47].

CONCLUSIONS

An effective and facile approach to the preparing a graft copolymerization of (St) monomer from PET surface was proved through TEMPO-mediated radical polymerization. The chemical structures of all specimens were identified using FTIR and ^{1}H NMR, DSC, TGA, TEM, and XRD. In addition, PET-*g*-PSt/MMT nanocomposite was synthesized by a solution intercalation method. Investigation of thermal properties using DSC and TGA manifested that the thermal stability and T_g of the nanocomposite partially increased compared to the pristine PET-g-PSt copolymer. These properties probably are due to an intense interplay between polymer matrix and silicate layers. TEM observation disclosed that silicate layers were randomly dispersed within the PET-*g*-PSt matrix, and multilayer morphology was destroyed and as a result, an exfoliated structure was observed for the prepared nanocomposite. In addition, according to the TEM image shown, a small number of clay layers tend to accumulate. Accordingly, it is noteworthy that the prepared PET-*g*-PSt copolymer and its attributed nanocomposite are likely to be used as amplifying agents in the preparation of composite polymers, as well as packaging and membrane materials owing to the combination of PSt and PET and synergetic performance of MMT.

ACKNOWLEDGEMENT

The authors earnestly express their gratitude to the Payame Noor University for supporting of this project.

CONFLICTS OF INTEREST

The authors declare that they have no conflicts of interest.

REFERENCES

1. Bech L, Elzein T, Meylheuc T, Ponche A, Brogly M, Telepoittevin B, Roger PH (2009) Atom transfer radical polymerization of styrene from different poly(ethylene terephthalate) surfaces: Films, fibers and fabrics. Eur Polym J 45: 246-255
2. Agranoff J (1984) Modern plastics encyclopedia, New York: McGraw Hill P: 106-180
3. Boxus T, Deldime-Rubbens M, Mougenot P, Schneider YJ, Marchand-Brynaert J (1996) Chemical assays of end-groups displayed on the surface of poly(ethylene terephthalate) (PET) films and membranes by radiolabeling. Polym Adv Technol 7: 589-598
4. Huang CJ, Chang TC (2004) Studies on the electromagnetic shielding effectiveness of metallized PVAc-$AgNO_3$/PET conductive films. J Appl Polym Sci 91: 270-273
5. Serad GE, Freeman BD, Stewart ME, Hill AJ (2001) Gas and vapor sorption and diffusion in poly(ethylene terephthalate). Polymer 42: 6929-6943
6. Gupta B, Plummera C, Bissonb I, Frey P, Hilborn J (2002) Plasma-induced graft polymerization of acrylic acid onto poly(ethylene terephthalate) films: Characterization and human smooth muscle cell growth on grafted films. Biomaterials 23: 863-871
7. Kishida A, Iwata H, Tamada Y(1991) Cell behaviour on polymer surfaces grafted with non-ionic and ionic monomers. Biomaterials 12: 786-792
8. Friebe A, Ulbricht M (2007) Controlled pore functionalization of poly(ethylene terephthalate) track-etched membranes via surface-initiated atom transfer radical polymerization. Langmuir 23: 10316-10322
9. Zhang HW, Shouro D, Itoh K, Takata T, Jiang Y (2008) Grafting polymer from poly(ethylene terephthalate) films by surface-initiated ATRP. J Appl Polym Sci 108: 351-357
10. Jia Z, Du SY, Tian GS (2007) Surface modification of acrylic fiber by grafting of casein. J Macromol Sci A 44: 299-304
11. Lim JG, Balk JH, Zhang XQ (2002) A novel preparation method of maleic anhydride grafted syndiotactic polystyrene and its blend performance

with nylon 6. Polym Bull 48: 397-405
12. Li HM, Chen HB, Shen ZG, Lin, Shangan (2002) Preparation and characterization of maleic anhydride-functionalized syndiotactic polystyrene. Polymer 43: 5455-5461
13. Blanchemain N, Halulon S, Martel B, Traisnelet M, Morcellet, M, Hildebrand, HF (2005) Vascular PET prostheses surface modification with cyclodextrin coating: Development of a new drug delivery system. Eur J Vasc Endovasc Surg 29: 628-632
14. Liu YX, He T, Gao CY (2005) Surface modification of poly(ethylene terephthalate) via hydrolysis and layer-by layer assembly of chitosan and chondroitin sulphate to construct cytocompatible layer for human endothelial cells. Colloids Surf B 46: 117-126
15. Ciobanu M, Siove A, Gueguen V, Gamble LJ, Castner DG, Migonney V (2006) Radical graft polymerization of styrene sulfonate on poly(ethylene terephthalate) films for ACL applications: "Grafting from" and chemical characterization. Biomacromolecule 7: 755-760
16. Ohe T, Yushimura Y, Abe I, Ikeda M, Shibutani Y (2007) Chemical introduction of sugars onto PET fabrics using diamine and cyanuric chloride. Text Res J 77: 131-137
17. Nasef MM (2000) Gamma radiation-induced graft copolymerization of styrene onto poly(ethylene terephthalate) films. J Appl Polym Sci 77: 1003-1012
18. Nasef MM (2002) Structural investigation of poly(ethylene terephthalate)-graft-polystyrene copolymer films. J Appl Polym Sci 84: 1949-1955
19. Rafiei H, Abbasian M, Yegani R (2020) Synthesis of well-defined poly(n-vinylpyrrolidone)/n-TiO_2 nanocomposites by xanthate-mediated radical polymerization. Iran Polym J 29: 371-381
20. Abbasian M, Bakhshi M, Jaymand M, Ghasemi Karaj-Abad S (2019) Nitroxide-mediated graft copolymerization of styrene from cellulose and its polymer/montmorillonite nanocomposite. J Elastom Plast 51: 473-489
21. Wang JS, Matyjaszewski K (2001) Controlled/living radical polymerization. Atom transfer radical polymerization in the presence of transition-metal complexes. J Am Chem Soc 117: 5614-5615
22. Abbasian M, Seyyedi M, Jaymand M (2020) Modification of thermoplastic polyurethane through the grafting of well-defined polystyrene and preparation of its polymer/clay nanocomposite. Polym Bull 77: 1107-1120
23. Benoit D, Chaplinski V, Braslau R, Hawker CJ (1999) Development of a universal alkoxyamine for living free radical polymerizations. J Am Chem Soc 121: 3904-3920
24. Wayland BB, Poszmik G, Mukerjee SL, Fryd M (1994) Living radical polymerization of acrylates by organocobalt porphyrin complexes. J Am Chem Soc 116: 7943-7944
25. Stenzel MH (2008) RAFT polymerization: An avenue to functional polymeric micelles for drug delivery. Chem Commun 30: 3486-3503
26. Fallah Iri Sofla S, Abbasian M, Mirzaei M (2019) Synthesis and micellar characterization of novel pH-sensitive thiol-ended triblock copolymer via combination of RAFT and ROP processes. Int J Polym Mater Po 68: 297-307
27. Abbasian M, Ghaeminia H, Jaymand M (2018) A facile and efficient strategy for the functionalization of multiple-walled carbon nanotubes using well-defined polypropylene-grafted Polystyrene. Appl Physics A 124: 1-9
28. Xu FJ, Neoh KG, Kang ET (2009) Bioactive surfaces and biomaterials via atom transfer radical Polymerization. Prog Polym Sci 34: 719-761
29. Abbasian M, Pakzad M, Amirmanesh M (2017) Polymericaly modified clays to preparation of polystyrene nanocomposite by nitroxide mediated radical polymerization and solution blending methods. Polym Compos 38: 1127-1134
30. Ghasemi Karaj-Abad S, Abbasian M, Jaymand M (2016) Grafting of poly(methyl methacrylate) -block-styrene onto cellulose via nitroxide-mediated polymerization, and its polymer/clay nanocomposite. Carbohydr Polym 152: 297-305
31. Kwan S, Maric M (2016) Thermoresponsive polymers with tunable cloud point temperatures grafted from chitosan via nitroxide mediated polymerization. Polymer 86: 69-82
32. Abreu CMR, Mendonca PV, Serra AC, Noble BB, Guliashvili JN, Coote ML, Coelho JFJ (2016) Nitroxide-mediated polymerization of vinyl chloride at low temperature: Kinetic and computa-

tional studies. Macromolecules 49: 490-498
33. Massoumi B, Abbasian M, Mohammad-Rezaei R, Amir Farnudiyan-Habibi A, Jaymand M (2019) Polystyrene-modified novolac epoxy resin/clay nanocomposite: Synthesis, and characterization. Polym Adv Technol 30: 1484-1492
34. Hawker CJ, Bosman AW, Harth, E (2001) New polymer synthesis by nitroxide mediated living radical polymerizations. Chem Rev 101: 3661-3688
35. Sanchez C, Soler-Illia GJ de AA, Ribot F, Lalot T, Mayer CR, Cabuild V (2001) Designed hybrid organic-inorganic nanocomposites from functional nanobuilding blocks. Chem Mater 13: 3061-3083
36. Suberlyak OV, Krasins'kyi VV, Moravs'kyi VV, Gerlach H, Jachowicz T (2014) Influence of aluminosilicate filler on the physicomechanical properties of polypropylene-polycaproamide composites. Mater Sci 50: 296-302
37. Jancar J, Douglas JF, Starr FW, Kumar SK, Cassagnau P, Lesser AJ, Sternstein SS, Buehler MJ (2010) Current issues in research on structure-property relationships in polymer nanocomposites. Polymer 51: 3321-3343
38. Yuvaraj J, Shim K, Taek L (2012) Synthesis of polymer-inorganic filler nanocomposites in supercritical CO_2. J Super Fluid 45: 71-63
39. Kiliaris P, Papaspyrides CD (2010) Polymer/layered silicate (clay) nanocomposites: an overview of flame retardancy. Prog Polym Sci 35: 902-958
40. Choudalakis G, Gotsis AD (2009) Permeability of polymer/clay nanocomposites: A review. Eur Polym J 45: 967-984
41. Majdzadeh-Ardakani K, Zekriardehani S, Coleman MR, Jabarin SA (2017) A novel approach to improve the barrier properties of PET/Clay nanocomposites. Int Polym Sci 2017: 7625906
42. Bech L, Elzein T, Meylheu T, Ponche A, Brogly M, Lepoittevin B, Roger P (2009) Atom transfer radical polymerization of styrene from different poly(ethylene terephthalate) surfaces: Films, fibers and fabrics. Eur Polym J 45: 246-255
43. Abbasian M (2007) Graft copolymerization of styrene onto PVC poly(vinyl chloride) and sPS (Syndiotactic Polystyrene) by living radical polymerization. PhD Thesis, Tabriz University
44. Jaymand M (2011) Exfoliated syndiotactic polystyrene-graft-poly(methyl methacrylate)/ montmorillonite nanocomposite prepared by solvent blending. Polymer 43:901-908
45. Xie HQ, Liu ZS, Guo JS (1994) Synthesis and properties of oxymethylene-linked oxyethylene-oxypropylene-styrene multiblock copolymers. Polymer 35: 4914-4919
46. Abbasian M, Shahparian M, Esmaeily Shoja Bonab S (2013) Chemical modification of polypropylene by nitroxide-mediated radical graft polymerization of styrene. Iran Polym J 22: 209-218
47. Longzhen Q, Wei C, Baojun Q (2005) Structural characterisation and thermal propertise of exfoliated polystyrene/ZnAl layered double hydroxide nanocomposites prepared via solution intercalation. Polym Degrad Stabil 87: 433-440